Self-Assembly, Structure, and Physical Properties of Tetranuclear Zn_{II} and Co_{II} Complexes of [2 × 2] Grid-Type

Javier Rojo,[a] Francisco J. Romero-Salguero,[a] Jean-Marie Lehn,*[a] Gerhard Baum,[b] and Dieter Fenske[b]

Keywords: Grid complexes / Self-assembly / Co / Zn / Coordination chemistry / Bis(tridentate) ligands

The tretrametallic [2 × 2] grid-type complexes **1–4** are formed by self-assembly of the bis(tridentate) ligands **5** and **6** with Zn^{II} and Co^{II} cations. They have been characterized by spectroscopic studies in solution as well as by crystal structure determination. The substituents in the central pyrimidine ring play an important role in terms of geometry and physical properties of the complexes. They induce an orthogonal orientation of the ligand in the complexes which is critical for the formation of ordered monolayers and extended self-organized arrays of grids. The physical properties of the complexes such as metal–metal interaction and π-π* stacking between the ligands may be modulated by changing these substituents.

Introduction

The self-assembly of suitable polydentate ligands with metal ions allows the preparation of well-defined inorganic supramolecular architectures in solution. In recent years, much effort has focused on the generation of inorganic arrays of various types in view of their promising physicochemical properties and their potential application in nanotechnology.[1−10]

The design of the ligand is the crucial for controlling the structure and properties of the final assemblies. Recently, our laboratory has reported the synthesis of bidentate ligands based on terpyridine subunits[11] and their self-assembly with metal ions of octahedral coordination to generate complexes of grid-type geometry.[12] The physicochemical properties of the [2 × 2] cobalt(II) grids formed indicate an electronic communication between the metallic centers suggesting that these inorganic assemblies could have applications in molecular information storage.[13] Moreover, the self-organization of such building blocks could lead to highly ordered monolayers[14] (e.g. "grids of grids") presenting magnetic domains or into which it might be possible to write information in the form of different metal redox states using for instance scanning probe microscopy techniques.

For generating such extended arrays, it is necessary that the basic grid components present regular, undistorted structures where the ligands are arranged in orthogonal fashion. Based on previous results, this arrangement depends in particular on the substituent present at the C^2 position of the pyrimidine ring.[15]

[a] Laboratoire de Chimie Supramoléculaire, ISIS − ULP − CNRS ESA-7006
4 rue Blaise Pascal, F-67000 Strasbourg, France
Fax: (internat.) + 33-3/88411020
E-mail: lehn@chimie.u-strasbg.fr
[b] Institut fur Anorganische Chemie, Universität Karlsruhe, D-76128 Karlsruhe, Germany

In the present work, we describe the formation as well as the structural and physico-chemical properties of the [2 × 2] grid-type complexes **1−4** obtained by the self-assembly of zinc(II) and cobalt(II) ions with the ligands **5** and **6** bearing a phenyl and a *p*-(dimethylamino)phenyl substituent, respectively, on the central pyrimidine (Scheme 1). The interaction between the phenyl ring and the pyridine units of the perpendicular ligands in the complexes induces an orthogonal arrangement suitable for applications in self-organizing systems.

Results and Discussion

Synthesis of Ligands 5 and 6 and of the Corresponding Grid Complexes 1−4

The synthesis of the bis(tridentate) ligand **5** has been reported previously.[11] Ligand **6** was obtained as described in Scheme 2. The reaction of equivalent amounts of ligands **5** or **6** and of the metal salts $Co(BF_4)_2$, $Co(DMSO)_4Tf_2$, or $ZnTf_2$ in acetonitrile leads to clear solutions from which the metal complexes **1−4** were isolated by precipitation with ethyl ether and centrifugation (**1** and **2**) or by simply removing the solvent under reduced pressure (**3** and **4**) (Scheme 1). These compounds were purified by recrystallization from acetonitrile/ethyl ether and characterized by physical and spectroscopic techniques as described below. The assembly rates of ligands **5** and **6** with Co^{II} and Zn^{II} ions to give complexes **1** and **2**, are appreciably slower than when the ligand does not present a phenyl substituent in the 2-position of the pyrimidine ring.[12] In the latter case, the self-assembly takes a few hours in contrast to the one night to two days for ligands **5** and **6**. This may be attributed to the steric hindrance introduced by the central phenyl substituent which must insert between two other ligands in the final grid complex (see below). All new compounds had spectral and analytical properties in agreement with their structure.

  1434−1948/99/0909−1421 $ 17.50+.50/0

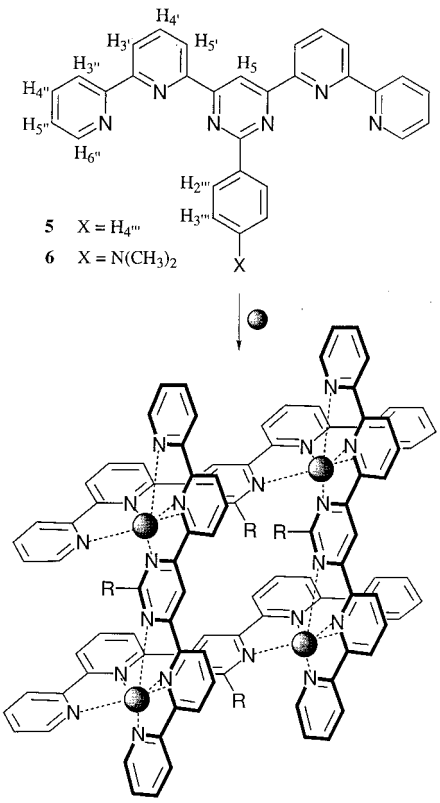

Scheme 1. Self-assembly of the [2 × 2] grid complexes **1**−**4** from the ligands **5**, **6**, and metal salts

^{1}H-NMR Spectra

The metal complexation leads to remarkable changes in the proton-NMR spectra with large modifications in the chemical shifts of the protons of the ligand. The metal binding induces a conformational change in the ligand. The most stable conformation of the ligand is that which adopts a *transoid* conformation around all C−C bonds linking the heterocyclic units;[11,16,17] in this form the nitrogen lone pairs of the heterocycle deshield the ligand protons adjacent to the interannular bonds (5-H, 5′-H, 3′-H, and 3′′-H). In the metal complex, the ligand presents a *cisoid* conformation to allow the formation of chelating coordination bonds with the metal centers and this deshielding effect disappears. The formation of the coordinative nitrogen−metal bonds as well as the positioning of the ligands in the complex also contribute to the chemical shift changes.

The proton-NMR spectra of ligand **5** and its Zn complex **1** as well as of ligand **6** and its Zn complex **3** are represented in Figures 1 and 2, respectively. The corresponding chemical shifts are listed in Table 1. The spectra of the cobalt(II) complexes **2** and **4** present special features due to the magnetic anisotropy effects of the ions; they will be described elsewhere.[18]

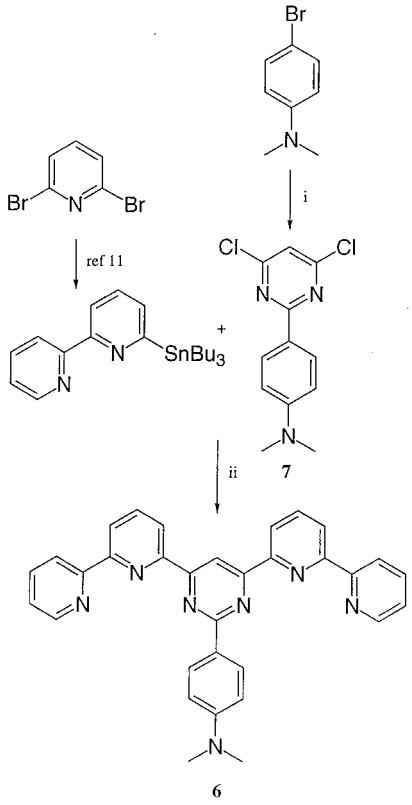

Scheme 2. Synthesis of the ligand **6**, i) *n*BuLi, THF, 4,6-dichloropyrimidine; ii) $Pd(Ph_3P)_4$, toluene

The major changes observed in the NMR spectra on complexation reside in the shielding of the phenyl protons. In the free ligand, these protons appear as a multiplet at low field corresponding to the *ortho* protons centered at δ = 8.78 and another multiplet centered at δ = 7.59 for the *meta* and *para* protons in the case of ligand **5** and an AA′BB′ system at δ = 8.79 and 6.87 for ligand **6**. The *ortho* protons are deshielded due to the presence of the two nitrogen lone pairs of the pyrimidine ring. When the zinc complexes **1** and **3** are formed, the multiplets are split into five and three well defined signals, respectively. The *ortho*, *ortho′* and *meta*, *meta′* protons of the phenyl ring, which are equivalent in ligands **5** and **6**, become nonequivalent in the complexes **1** and **3**. Moreover, all the aromatic protons are markedly shielded giving signals between δ = 7.0 and 4.96. These two observations suggest that in solution the complexes **1** and **3** adopt a very compact structure where the phenyl rings of the two ligands on one face of the grid structure insert between the two ligands on the other face. As a result, the phenyl protons are subject to strong shielding effects due to the heteocyclic units, thus inducing large shifts; furthermore, rotation around the phenyl−pyrimidine C−C bond is blocked, leading to nonequivalence of the *o*, *o′* and *m*, *m′* protons. This has been confirmed by a ROESY NMR experiment where a NOE interaction between 3′′′-H and 3′-H and 4′-H as well as between 3′′′-H^i and 5-H and 5′-H is observed for complex **1**.

In the Zn complex **3**, the signal of the methyl substituents on the amino group appears as a broad resonance centered

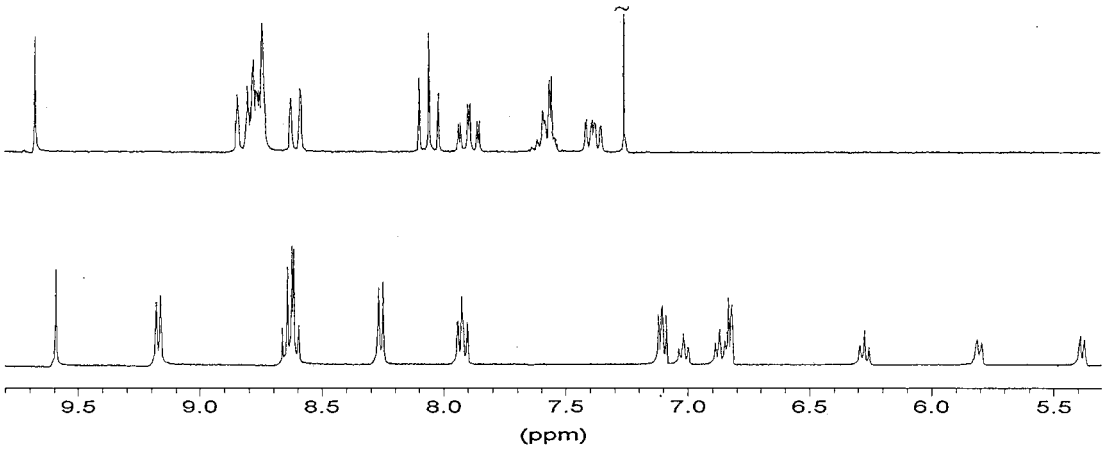

Figure 1. Proton-NMR spectra of ligand **5** at 200 MHz in $CDCl_3$ (top) and the Zn_4 complex **1** at 400 MHz in CD_3CN (bottom); for signal assignments, see Experimental Section

Table 1. Chemical shifts and chemical shift differences for proton-NMR signals of cornplexes **1** and **3** (in CD_3CN) and ligands **5** and **6** (in $CDCl_3$)[a]

Compound	5-H	5′-H	4′-H	3′-H	3′′-H	4′′-H	5′′-H	6′′-H	2′′′-H^o	2′′′-H^i	3′′′-H^o	3′′′-H^i	4′′′-H
5	9.69		8.08		8.84	7.91	7.40	8.76	8.78	8.78	7.59	7.59	7.59
1	9.57	9.17	8.63	8.63	8.25	7.92	7.10	6.82	5.80	5.38	7.00	6.27	6.87
Δδ	−0.12		+0.55		−0.59	+0.01	−0.30	−1.94	−2.98	−3.40	−0.59	−1.32	−0.72
6	9.54		8.07			7.91	7.38	8.79	8.79	8.79	6.87	6.87	
3	9.67	9.29	8.54	8.61		7.90	7.09	6.86	5.34	5.49	4.96	5.49	
Δδ	+0.13		+0.47			−0.01	−0.29	−1.93	−3.45	−3.30	−1.91	−1.38	

[a] *i* and *o* designate the inner and outer *ortho* and *meta* protons, respectively, on the phenyl substituent.

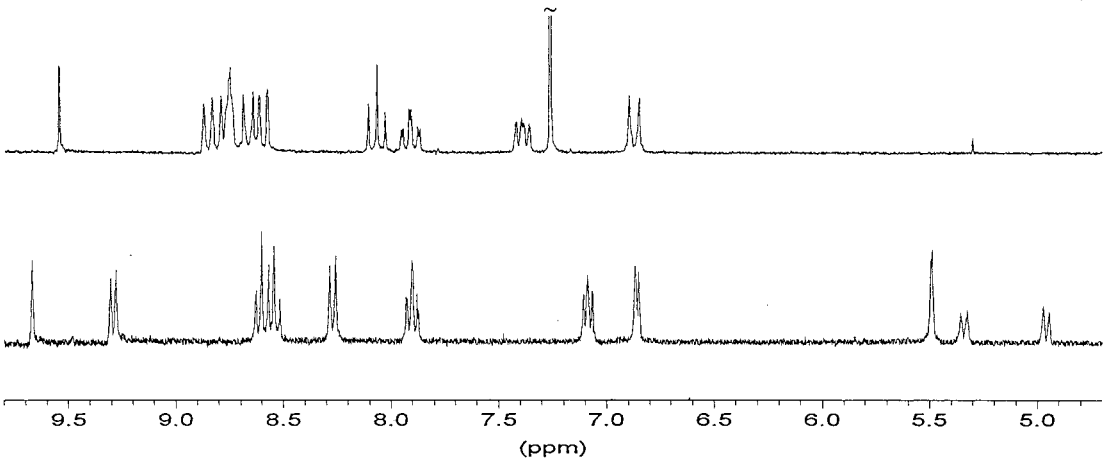

Figure 2. Proton-NMR spectra of ligand **6** at 200 MHz in $CDCl_3$ (top) and the Zn_4 complex **3** at 300 MHz in CD_3CN (bottom); for signal assignments, see Experimental Section

at δ = 3.07 in the proton-NMR spectrum. Due to the complex structure the rotation around the N−C bond is hindered. A variable-temperature experiment was performed (Figure 3). When the sample was heated to 333 K the broad band sharpened to a fine singlet for the two chemically equivalent methyl groups. When the temperature was lowered to 243 K, the signal at δ = 3.07 split into two singlets at δ = 3.25 and 2.88. A NOESY experiment allowed the assignment of the low-field peak as the signal of internal methyl group and the other one of the external methyl group. With a coalescence temperature T_c of 290 K a free energy of activation $\Delta G_c^{\geq}$ for the rotation around the N−C bond may be calculated as $\Delta G_c^{\geq} = 4.57T_c\cdot(9.97 + \log T_c/\delta\nu)$ where δν is the chemical shift difference between the two signals,[19] giving a value of 13.6 kcal/mol.

In this variable-temperature experiment the other signals in the spectrum did not change except those corresponding to the phenyl ring which may be affected by small changes in the complex structure with temperature. The data also show that at the highest temperature reached, rotation of

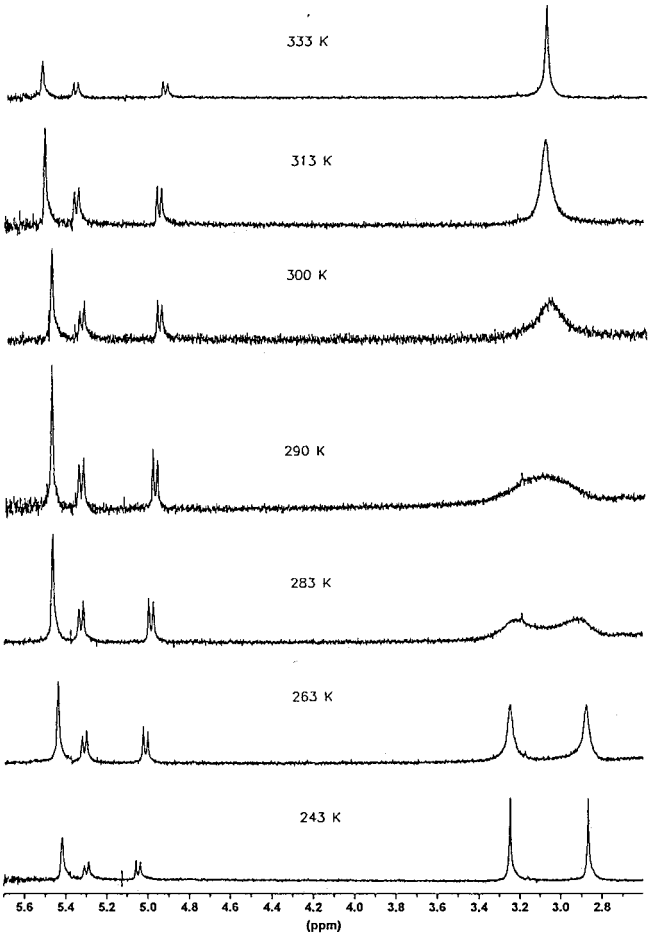

Figure 3. Proton-NMR spectra at different temperatures for the Zn_4 complex **3** at 300 MHz in CD_3CN (heteroaromatic protons not shown)

the phenyl group with respect to the pyrimidine ring is still slow on the NMR time scale, indicating that no significant dissociation of the complex is taking place. One may note that the phenyl ring rotation is thus a probe for investigating the kinetics of ligand exchange in such grid complexes.[18]

Crystal Structures of the Complexes 1, 2, and 4

The structures of the Zn^{II} and Co^{II} complexes **1**, **2**, and **4** of ligands **5** and **6** were investigated by X-ray crystallography. Those of **1** and **2** are represented in Figures 4 and 5. In all three structures the complexes present a [2 × 2] grid-type architecture in which the four metal ions form a square and lie close to an average common plane.

In the complex $\{[\mathbf{5}_4Zn_4](CF_3SO_3)_8\}$ (**1**) the Zn^{II} ions display a distorted octahedral coordination (Figure 4). The Zn−Zn distances lie in the range of 6.584−6.767 Å. The Zn−N bond lengths are between 2.053 and 2.184 Å for the pyridine nitrogen atoms and between 2.231 and 2.373 Å for the pyrimidine nitrogen atoms. The distances between the heteroaromatic rings of one ligand and the phenyl ring of the orthogonal one (3.25−3.50 Å) indicate van der Waals contact and π−π stacking interaction.

The complex $\{[\mathbf{5}_4Co_4](BF_4)_8\}$ (**2**) crystallizes with two molecules per unit cell. The metal ions also display a distorted octahedral coordination with Co,Co distances between 6.453−6.570 Å (Figure 5). The Co−N bond lengths lie between 2.041−2.175 Å for pyridine nitrogens and are slighly longer (2.213−2.309 Å) for the pyrimidine nitrogens. Again the short distances between phenyl and pyridine rings indicate π, π stacking.

In the case of $\{[\mathbf{6}_4Co_4](CF_3SO_3)_8\}$ (**4**), the overall quality of the crystal structure data is at this stage too low for a detailed description. However, the analysis indicates without doubt the [2 × 2] grid-type arrangement. Crystals of better quality are required for improving the structural data.

The central substituent in position 2 of the pyrimidine ring plays an important role in the geometrical features of the final complexes. It has been shown that in the case of rack-type metal ion coordination arrays, a methyl substituent was the best suited for the formation of complexes presenting the least distorted ligand geometry.[15] In the case of a cobalt(II) [2 × 2] grid complex of the type studied here, the presence of a methyl substituent on the central pyrimidine ring was found to cause a divergent, outward bending of the planes of the ligands, a CH_3 group being apparently somewhat too large.[12] On the contrary, when there is no substituent in that position, the situation is opposite and an inward, convergent bending is observed in the corresponding $(Zn^{II})_4$ complex.[20] An intermediate situation is found in the present case of a phenyl substituent which has a thickness intermediate between the steric requirements of CH_3 and H. Insertion of the phenyl group between two ligands in complexes **1** and **2** induces an almost parallel arrangement of the average planes of the ligands, thus leading to an overall geometry of the [2 × 2] grid complexes close to a regular square (Figures 4 and 5).

UV/Vis Absorption and Emission Spectra

The absorption maxima (λ_{max}) and extinction coefficients (ε) for ligands **5** and **6** in chloroform and for complexes **1**, **2**, **3**, and **4** in acetonitrile are listed in Table 2. The UV region of the absorption spectra shows strong absorption bands at 280−290 and 350−375 which correspond to ligand-centered (LC) π-π* transition bands. In the ligands, these bands appear at higher energies.

In the case of complexes **2**, **3**, and **4**, absorption bands are observed in the visible region. The zinc complex **3** presents a remarkable deep red color, corresponding to an intense absorption band at 516 nm which could be due to a donor-acceptor charge transfer transition between the electron-rich (dimethylamino)phenyl group and the pyridine rings held in stacking position by the structure of the complex. The broad bands centered between 400−475 and 532 nm in the Co complexes **2** and **4**, respectively, could correspond to Co^{II}−bipyridine MLCT and the very broad

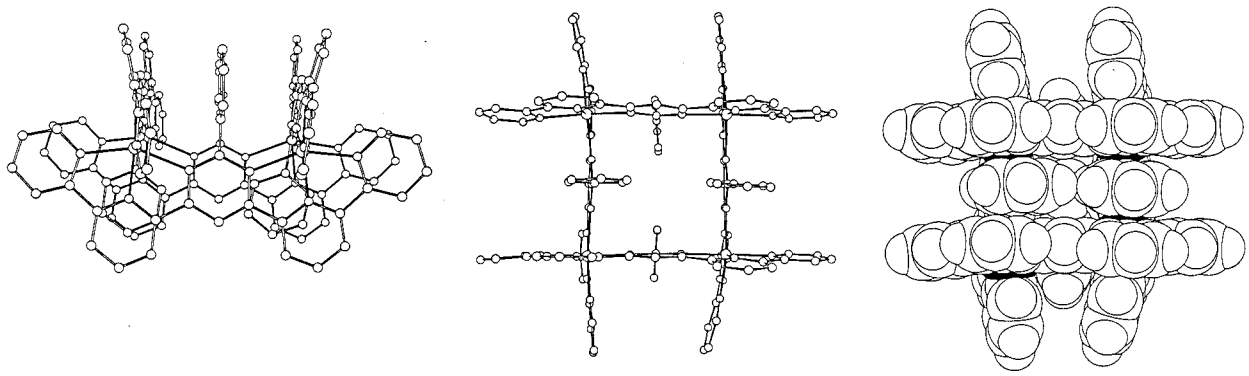

Figure 4. X-ray structure of the [2 × 2] Zn_4 grid complex **1**: side view (left); top view (center); top view, space-filling representation (right)

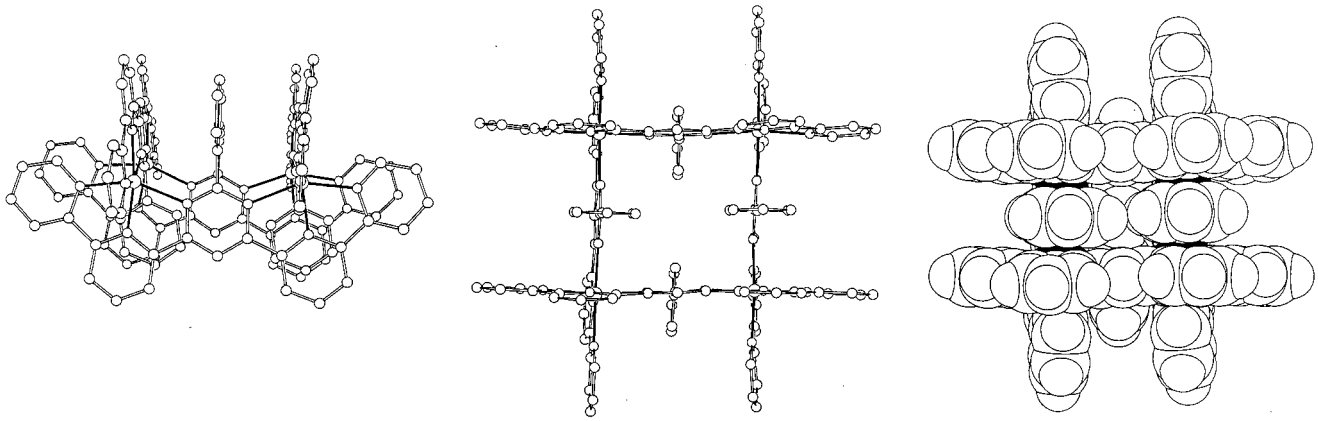

Figure 5. X-ray structure of the [2 × 2] Co_4 grid complex **2**: side view (left); top view (center); top view, space-filling representation (right); this is one of the two grid complexes present in the unit cell

Table 2. Electronic absorption spectral data for the complexes **1**–**4** and the ligands **5** and **6** in acetonitrile, λ in nm (ε in 10^4 $M^{-1}cm^{-1}$)

Compound		π-π* (LC)
5		333 (1.0), 332 (1.4), 284 (3.5), 274 (3.8), 256 (3.2), 236 (4.8)
1		375 (6.5), 358 (7.2), 294 (4.2), 282 (4.9)
2	430 (0.1)[a]	371 (0.8), 361 (0.9), 291 (0.7), 279 (18)
6	402 (0.7)[b]	348 (8.4), 312 (7.9), 284 (10.0)
3	516 (5.5)[b]	371 (1.3), 357 (1.3), 295 (0.8), 282 (0.9), 261 (1.3)
4	532 (1.1)[a]	365 (18.5), 292 (13.2), 267 (19.8)

[a] Metal-to-ligand charge-transfer transitions. – [b] Ligand-centered transitions, probably of donor-acceptor type for **3**.

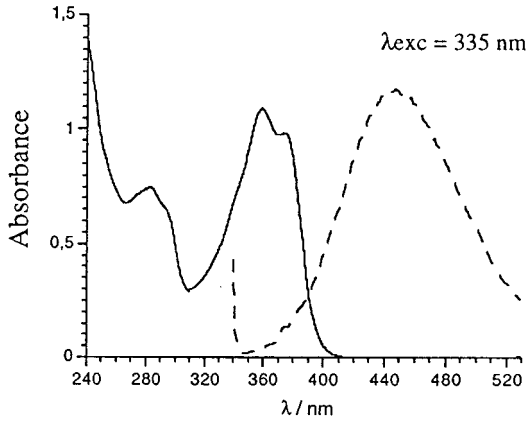

Figure 6. Electronic absorption and emission (broken line) spectra of the Zn_4 grid complex **1** in acetonitrile

shoulder at lower energy to Co^{II}–pyrimidine MLCT transitions.

The strong fluorescence of the zinc complex **1** is noteworthy. Whereas ligand **5** in chloroform exhibits only a weak emission at about 410 nm when irradiated at 272 nm, complex **1** in acetonitrile presents an intense emission at 450 nm under excitation at 335 nm at room temperature (Figure 6).[21] Since the Zn^{II} ions are of d^{10} electronic configuration and possess no low-lying metal-centered excited states, the fluorescence of **1** may be ascribed to emission from the lowest ligand-centered excited singlet level, its high intensity being due to the rigidity of the complex, which decreases the radiationless decay relative to that for the free ligand **5**. The absence of emission for the cobalt complex **2** is due to the presence of the low-lying nonemissive Co^{II}-centered MLCT excited state which inhibits luminescence,

as has been previously observed for other cobalt complexes.[22] Ligand **6** and its metal complexes **3** and **4** show no emission. Radiationless decay of the ligand-centered levels may take place in **3** and **4** through the low-energy charge transfer and MLCT excited states.

Electrochemical Properties

Preliminary studies indicated that the present grid-type species, in particular the Co^{II} complexes **2** and **4** present remarkable electrochemical properties, in line with those reported earlier for the related $(Co^{II})_4$ grid bearing no phenyl group on the pyrimidine rings.[12] Thus, for instance, eight successive reductions are observed for **2** at about −0.10, −0.24, −0.45, −0.77, −1.00, −1.22, −1.38, and −1.54 V (in DMF). Similar values are also found for **4**. Detailed investigations are in progress and will be reported together with data on related complexes.

Conclusion

The formation of the four tetrametallic complexes **1**−**4** from the ligands **5** and **6** and Co^{II} and Zn^{II} metal ions with octahedral coordination confirms the generality of the self-assembly of such grid-type architectures. The stacking interactions introduced by the phenyl ring provide high stability to the complexes as well as structural features suitable for their use as components in extended self-organized arrays. The introduction of an electron-donating group on the phenyl ring provides means for modulating the electronic properties of the ligand and therefore the properties of the final complexes. The control which may thus be progressively achieved over both the structural and electronic features of these tetrametallic grid complexes makes them particularly attractive as components in the construction of inorganic architectures for multicellular ion-dot supramolecular devices.

Experimental Section

Materials: Precipitates were isolated by high-speed spinning in a Hettich Universal centrifuge (ca. 3000 rpm, 5 min). − Unless otherwise noted, ^{1}H-NMR spectra were measured in CD_3CN calibrated to the residual solvent peak at 200 MHz with a Bruker AC 200 spectrometer. − Melting points were obtained with a digital Thomas Hoover (Electrotherma) apparatus. − Infrared absorption spectra were recorded on a Perkin−Elmer 1600 series FTIR spectrometer in KBr, an electronic absortion espectra on a Cary 219 spectrometer in CH_3CN with λ_{max} in nm and ε ($\times 10^4$) in M^{-1} cm^{-1}. − Fast atom bombardment (FAB) mass spectrometry was performed on a ZAB-HF VG spectrometer with *m*-nitrobenzyl alcohol as the matrix and electrospray (ES) mass spectra were obtained with a triple quadrupole mass spectrometer Quattro II (Micromass) mass spectrometry. Spectroscopic studies were performed in spectroscopic-grade solvents. − All solvents were reagent-grade and used without further purification.

Complex $(5_4Zn_4)(CF_3SO_3)_8$ (1): To a suspension of 4,6-bis(2′′,2′-bipyrid-6′-yl)-2-phenylpyrimidine[11] (20 mg, 0.043 mmol) in acetonitrile (6 mL) was added zinc triflate (16 mg, 0.043 mmol) and the mixture was stirred at room temperature for 18 h. Diethyl ether was added to the reaction and the precipitate was isolated by centrifugation and purified by recrystallization from acetonitrile/diethyl ether to afford **1** as a white solid (22 mg, 63%). − M.p. > 300 °C. − ^{1}H NMR (400 MHz): δ = 9.57 (s, 1 H, 5-H), 9.17 (d, 2 H, *J* = 6.3 Hz, 5′-H), 8.63 (m, 4 H, 4′-H, 3′-H), 8.25 (d, 2 H, *J* = 8.2 Hz, 3′′-H), 7.92 (t, 2 H, *J* = 7.7 Hz, 4′′-H), 7.10 (dd, 2 H, *J* = 6.5, 5.2 Hz, 5′′-H), 7.00 (t, 1 H, *J* = 7.4 Hz, 3′′′-H^i), 6.87 (t, 1 H, *J* = 7.6 Hz, 4′′′-H), 6.82 (d, 2 H, *J* = 5.2 Hz, 6′′-H), 6.27 (t, 1 H, *J* = 7.6 Hz, 3′′′-H), 5.80 (d, 1 H, *J* = 7.2 Hz, 2′′′-H^i), 7.38 (d, 1 H, *J* = 7.6 Hz, 2′′′-H). − FAB MS; *m*/*z* (%): 3123 (2) [*M* − 149 (− Tf)], 3014 (7) [*M* − 298 (− 2 Tf)], 2863 (8) [*M* − 447 (− 3 Tf)], 2714 (5) [*M* − 596 (−4 Tf)], 2566 (3) [*M* − 745 (−5 Tf)]. − $C_{128}H_{80}F_{24}N_{24}O_{24}S_8Zn_4$ (3312.17): calcd. C 46.42, H 2.43, N 10.15; found C 46.46, H 2.15, N 10.04. − IR (KBr): $\tilde{\nu}$ = 3089, 1600, 1465, 1256, 1162, 1029, 776, 637. − UV/Vis: λ (ε_{max}) = 282 (4.9), 294 (4.2), 358 (7.2), 375 (6.5).

Complex $(5_4Co_4)(BF_4)_8$ (2): To a suspension of 4,6-bis(2′′,2′-bipyrid-6′-yl)-2-phenylpyrimidine[11] (20 mg, 0.043 mmol) in acetonitrile (6 mL) was added cobalt tetrafluoroborate (15 mg, 0.043 mmol) and the mixture was stirred at reflux for 2 d. Diethyl ether was added to the reaction and the precipitate was isolated by centrifugation and purified by recrystallization from acetonitrile/diethyl ether to afford **2** as a slightly brown solid (23 mg, 77%). − M.p. > 300 °C. − FAB MS; *m*/*z* (%): 2701 (20) [*M* − 87 (− BF_4)], 2614 (81) [*M* − 174 (− 2 BF_4)], 2528 (95) [*M* − 261 (− 3 BF_4)], 2441 (48) [*M* − 348 (− 4 BF_4)], 2354 (16) [*M* − 435 (− 5 BF_4)], 1307 (37) [{*M* − 174 (− 2 BF_4)}/2], 1264 (100) [{*M* − 261 (− BF_4)}/2], 1220 (83) [{*M* − 348 (− 4 BF_4)}/2]. − $C_{120}H_{80}B_8Co_4F_{32}N_{24}$ (2788.31): calcd. C 51.69, H 2.89, N 12.06; found C 51.47, H 2.90, N 11.87. − IR (KBr): $\tilde{\nu}$ = 3072, 1600, 1463, 1228, 773, 656. − UV/Vis: λ (ε_{max}) = 279 (1.8), 291 (0.7), 361 (0.9), 371 (0.8), 430 (0.1).

4,6-Dichloro-2-[4′-(dimethylamino)phenyl]pyrimidine (7): To *p*-bromo(dimethylamino)benzene (5 g, 24.988 mmol) in ethyl ether (80 mL) at room temperature under argon was added one equiv. of 1.6 M *n*BuLi in hexane (15.6 mL, 24.988 mmol). The mixture was stirred for 5 min and then cooled at −70 °C. Then, one equiv. of 4,6-dichloropyrimidine (3.7 g, 24.988 mmol) was added. After 1 h 15 min, the temperature of the mixture was allowed to rise to 0 °C, a solution of acetic acid, water, and THF (1.6:0.25:5 mL) was added dropwise, and the mixture was immediately treated with a solution of DDQ (5.9 g, 26 mmol) in THF (25 mL). The solution was stirred at room temperature for 15 min, cooled to 0 °C and a cold 3 M aqueous solution of NaOH (10 mL, 30 mmol) was added followed by water (10 mL) 15 min later. The organic phase was removed and the aqueous layer was extracted with chloroform (5 × 100 mL). The combined organic layers were dried (Na_2SO_4) and the solvent was removed under low pressure. The residue was purified by chromatography on silica gel using hexane/ethyl acetate (6:1) as eluent giving 1.33 g (20% yield) of **7** as yellow needles. − M.p. 174−175 °C. − ^{1}H NMR: δ = 8.29 (d, 2 H, *J* = 8.9 Hz, Ar), 7.06 (s, 1 H, 4-H), 6.71 (d, 2 H, *J* = 8.9 Hz, Ar), 3.07 [s, 6 H, $(CH_3)_2N$]. − ^{13}C NMR: δ = 166.1, 161.5, 153.1, 130.5, 122.2, 116.2, 111.3, 40.1. − EI MS; *m*/*z* (%): 269 (64) [M^+ + 1], 268 (14) [M^+], 267 (100) [M^+ − 1]. − $C_{12}H_{11}Cl_2N_3$ (268.14): calcd. C 53.93, H 4.15, N 15.73; found C 53.65, H 4.05, N 15.71. − IR (KBr): $\tilde{\nu}$ = 3109, 2899, 1609, 1536, 1385, 1190, 1093, 819, 778.

4,6-Bis(2′′,2′-bipyrid-6′-yl)-2-[4′′-(dimethylamino)phenyl]pyrimidine (6): To 4,6-dichloro-2-[4′-(dimethylamino)phenyl]pyrimidine (**7**) (250 mg, 0.9323 mmol), 1.5 equiv. of 6-tributylstannyl-2,2′-

bipyridine[11] (622 mg, 1.3984 mmol) and 10% of tetrakis(triphenylphosphane)palladium (0) (108 mg, 0.0932 mmol) was added toluene (15 mL) and the mixture was refluxed overnight under argon. Then, the solvent was removed under low pressure and the residue was washed with MeOH (10 mL). Without further purification, again 1.5 equiv. of 6-tributylstannyl-2,2′-bipyridine (622 mg, 1.3984 mmol), 10% of tetrakis(triphenylphosphane)palladium(0) (108 mg, 0.0932 mmol), and toluene (15 mL) were added to the solid. The mixture was heated at reflux for 24 h under argon. The solvent was removed and the slurry residue was treated with MeOH (10 mL). The solid was filtered and washed with more MeOH (10 mL) to give 230 mg (53%) of **6** as a yellow solid. − M.p. 302−304 °C (calcination). − ^{1}H NMR: δ = 9.54 (s, 1 H, 5-H), 8.85 (d, 2 H, *J* = 7.9 Hz, 3′′-H), 8.79 (m, 4 H, 6′′-H, Ar), 8.66 (d, 2 H, *J* = 8.9 Hz, 3′-H or 5′-H), 8.59 (d, 2 H, *J* = 7.8 Hz, 3′-H or 5′-H), 8.07 (t, 2 H, *J* = 7.8 Hz, 4′-H), 7.91 (dt, 2 H, *J* = 7.8, 1.8 Hz, 4′′-H), 7.38 (dd, 2 H, *J* = 6.7, 4.9 Hz, 5′′-H) 6.87 (d, 2 H, *J* = 9 Hz, Ar), 3.11 (s, 6 H, 2× CH_3). − ^{13}C NMR: δ = 172.7, 163.9, 158.1, 155.5, 149.2, 137.9, 136.7, 129.7, 129.5, 123.9, 122.7, 122.2, 121.7, 121.3, 121.0, 111.7, 110.1, 40.3. − MS (FAB); *m*/*z*: 508 [M^+ + 1]. − HRMS: $C_{32}H_{26}N_7$: calcd. 508.2250, found: 508.2235. − UV/Vis: λ(ε_{max}) = 284 (10.0), 312 (7.9), 348 (8.4); 402 (0.7). − The reaction was tried in a single step using double amount of reagents but only poor yields were obtained.

Complex $(6_4Zn_4)(CF_3SO_3)_8$ (3): To a suspension of 4,6-bis(2′′,2′-bipyrid-6′-yl)-2-[4′′-(dimethylamino)phenyl]pyrimidine (**6**) (20 mg, 0.039 mmol) in acetonitrile (8 mL) was added zinc triflate (14 mg, 0.039 mmol) and the mixture was refluxed for 48 h under argon. The solvent was removed under low pressure and the solid recrystallized from acetonitrile/diethyl ether to afford **3** as a deep red solid (27 mg, 79%). − M.p. > 300 °C. − ^{1}H NMR (300 MHz): δ = 9.67 (s, 1 H, 5-H), 9.29 (d, 2 H, *J* = 7.4 Hz, 5′-H), 8.61 (d, 2 H, *J* = 7.5 Hz, 3′-H), 8.54 (t, 2 H, *J* = 8.1 Hz, 4′-H), 8.27 (d, 2 H, *J* = 8.2 Hz, 3′′-H), 7.90 (dt, 2 H, *J* = 7.8, 1.6 Hz, 4′′-H), 7.09 (dd, 2 H, *J* = 7.6, 6.1, 5′′-H), 6.86 (d, 2 H, *J* = 5.2 Hz, 6′′-H), 5.49 (S_b, 2 H, 2′′-H^i, 3′′′-H^i), 5.34 (d, 1 H, *J* = 9.0 Hz, 2′′′-H), 4.96 (d, 1 H, *J* = 8.0 Hz, 3′′′-H), 3.07 (S_b, 6 H, 2 × CH_3). − ES MS; *m*/*z*: 1593.7 [M − 298 (− 2 Tf)], 1012.6 [M − 447 (− 3 Tf)], 720 [M − 596 (− 4 Tf)]. − $C_{136}H_{100}F_{24}N_{28}0_{24}S_8Zn_4$ (3484.45): calcd. C 46.88, H 2.89, N 11.26; found C 47.12, H 3.06, N 11.00. − UV/Vis: λ(ε_{max}) = 261 (1.3), 282 (0.9), 295 (0.8), 357 (1.3), 371 (1.3), 516 (5.5).

Complex $(6_4Co_4)(CF_3SO_3)_8$ (4): To a suspension of 4,6-bis(2′′,2′-bipyrid-6′-yl)-2-[4′′-(dimethylamino)phenyl]pyrimidine (**6**) (10 mg, 0.0197 mmol) in acetonitrile (5 mL) was added cobalt triflate tetrakis(DMSO) (16 mg, 0.0197 mmol) and the mixture was refluxed for 48 h under argon. The solvent was removed under low pressure and the solid recrystallized from acetonitrile/diethyl ether to afford **4** as a dark solid (10 mg, 60%). − M.p. > 300 °C. − FAB MS; *m*/*z* (%): 3309.7 (4) [M − 149 (− Tf)], 3159.4 (9) [M − 298 (− 2 Tf)], 3010.5 (7) [M − 447 (− 3 Tf)], 2861.6 (3) [M − 596 (− 4 Tf)], 2713.5 (1) [M − 745(− 5 Tf)]. − $C_{136}H_{100}Co_4F_{24}N_{28}O_{24}S_8$ (3458.66): calcd. C 47.23, H 2.91, N 11.34; found C 47.49, H 2.62, N 11.31. − UV/Vis: λ(ε_{max}) = 267 (19.8), 292 (13.2), 365 (18.5), 532 (1.1).

Crystal Structure Determinations: The measurements were carried out with a STOE-IPDS diffractometer with graphit-monochromatized Mo-K_α radiation. Table 3 summarizes the crystal data, data collection, and refinement parameters. All calculations were performed with the SHELX-97 package.[24] All structures were solved by direct methods and were refined by full-matrix least squares based on F^2. All hydrogen atoms, disordered anions and solvent molecules with an occupation factor less than 1.0 were refined isotropically. All of the C−H hydrogen atoms in all structures were placed in calculated positions with U(H) = 1.5U_{eq}(C) for methyl groups and U(H) = 1.2U_{eq}(C) for all other. Molecular graphics performed with SCHAKAL96.[25] Single crystals of the complexes were obtained by slow vapor diffusion of diethyl ether into aceto-

Table 3. Crystal data and structure refinement for complexes **1** and **2**

	Complex **1**	Complex **2**
Empirical formula	$C_{120}H_{80}N_{24}Zn_4{\cdot}(SO_3CF_3)_8{\cdot}(MeCN)_{4.5}$	$C_{120}H_{80}N_{24}Co_4{\cdot}8BF_4{\cdot}13.5MeCN{\cdot}0.75Et_2O{\cdot}0.5H_2O$
M_r [g mol^{-1}]	3496.86	3407.10
T [K]	198(1)	200(1)
Wavelength [Å]	0.71073	0.71073
Crystal system	monoclinic	triclinic
Space group	*C*2/*c*	*P*1bar
a [Å]	53.751(11)	18.118(4)
b [Å]	20.281(4)	27.476(6)
c [Å]	30.748(6)	32.602(7)
α [°]	90	97.54(3)
β [°]	120.02(3)	100.33(3)
γ [°]	90	98.03(3)
Volume [Å]	29023(10)	15605(5)
Z	8	4
$\rho_{calcd.}$ [g cm^{-3}]	1.601	1.45
μ(Mo-K_α [mm^{-1}]	0.879	0.521
F(000)	14168	6950
Crystal size [mm]	0.20 × 0.15 × 0.10	0.30 × 0.20 × 0.20
Θ [°]	2.05 − 25.05	1.87−25.07
Index ranges	$-63 \le h \le 54$, $-24 \le k \le 24$, $-29 \le l \le 36$	$-21 \le h \le 21$, $-31 \le k \le 32$, $-38 \le l \le 33$
Reflections collected	58633	76177
R(int)	0.0430	0.0581
Independent reflections	24149	49669
Data/restraints/parameters	24149/885/2140	49669/2350/4262
GoF *S*	1.382	1.023
Final *R* indices [$I > 2\sigma(I)$]	R_1 = 0.0678, wR_2 = 0.1845	R_1 = 0.0761, wR_2 = 0.2159
R indices (all data)	R_1 = 0.0884, wR_2 = 0.1955	R_1 = 0.0945, wR_2 = 0.2346
Largest diff. peak/hole [eÅ^{-3}]	1.637/−1.208	1.745/−0.807

nitrile solutions. The Zn^{II} complex **1** crystallized with several acetonitrile molecules. The dark brown crystals of the Co^{II} complex **2** contained several solvent molecules (CH_3CN, Et_2O, and H_2O). Crystallographic data (excluding structure factors) for the structures of complexes **1** and **2** have been deposited with the Cambridge Crystallographic Data Centre as supplementary publication no. CCDC-120674 for **1** and -120673 for **2**. Copies of the data can be obtained free of charge on application to CCDC, 12 Union Road, Cambridge CB2 1EZ, UK [Fax: + 44-1223/336-033; E-mail: deposit@ccdc.cam.ac.uk].

Acknowledgments

We thank the French Goverment (J. R.) and the Ministerio de Educación y Ciencia (Spain) (F. J. R. S.) for postdoctoral fellowships. We also thank Hélène Nierengarten and Emmanuelle Leize for the ESMS determinations, Patrick Maltèse for the NOESY NMR experiments, and Mario Ruben for some spectroscopic measurements.

[1] *Comprehensive Supramolecular Chemistry* (Eds.: J. L. Atwood, J. E. D. Davies, D. D. MacNicol, F. Vögtle, J.-M. Lehn), Pergamon, Oxford, **1996**; P. N. W. Baxter, vol. 9, pp. 166−211; E. C. Constable, vol. 9, pp. 213−252; M. Fujita, vol. 9 pp. 254−282.
[2] E. C. Constable, *Progress in Inorganic Chemistry* (Ed.: K. D. Karlin), John Wiley and Sons, New York, **1994**, vol. 42, pp. 67−138.
[3] J.-M. Lehn, *Supramolecular Chemistry: Concepts and Perspectives*, VCH, Weinheim, **1995**, chapter 9.
[4] P. N. W. Baxter, J.-M. Lehn, J. Fischer, M.-T. Youinou, *Angew. Chem.* **1994**, *106*, 2432; *Angew. Chem. Int. Ed. Engl.* **1994**, *33*, 2284.
[5] B. Hasenknopf, J.-M. Lehn, B. O. Kneisel, G. Baum, D. Fenske, *Angew. Chem.* **1996**, *108*, 1987; *Angew. Chem. Int. Ed. Engl.* **1996**, *36*, 1838.
[6] P. N. W. Baxter, G. S. Hanan, J.-M. Lehn, *J. Chem. Soc., Chem. Commun.* **1996**, 2019.
[7] B. Hasenknopf, J.-M. Lehn, G. Baum, D. Fenske, *Proc. Natl. Acad. Sci. USA* **1996**, *93*, 1397
[8] B. Hasenknopf, J.-M. Lehn, N. Boumediene, A. Dupont-Gervais, A. Van Dorsselaer, B. Kneisel, D. Fenske, *J. Am. Chem. Soc.* **1997**, *119*, 10956.
[9] D. P. Funeriu, J.-M. Lehn, G. Baum, D. Fenske, *Chem. Eur. J.* **1997**, *3*, 99.
[10] E. C. Constable, A. M. W. Cargill-Thompson, P. Harveson, L. Macko, M. Zehnder, *Chem. Eur. J.* **1995**, *1*, 360.
[11] G. S. Hanan, U. S. Schubert, D. Volkmer, E. Rivière, J.-M. Lehn, N. Kyritsakas, J. Fischer, *Can. J. Chem.* **1997**, *75*, 169.
[12] G. S. Hanan, D. Volkmer, U. S. Schubert, J.-M. Lehn, G. Baum, D. Fenske, *Angew. Chem.* **1997**, *109*, 1929; *Angew. Chem. Int. Ed. Engl.* **1997**, *36*, 1842.
[13] O. Waldmann, J. Hassmann, P. Müller, G. S. Hanan, D. Volkmer, U. S. Schubert, J.-M. Lehn, *Phys. Rev. Lett.* **1997**, *78*, 3390.
[14] I. Weissbuch, P. N. W. Baxter, S. Cohen, K. Kjaer, P. B. Howes, J. Als-Nielsen, G. S. Hanan, U. S. Schubert, J.-M. Lehn, L. Leiserowitz, M. Lahav, *J. Am. Chem. Soc.* **1998**, *120*, 4850.
[15] G. S. Hanan, C. R. Arana, J.-M. Lehn, G. Baum, D. Fenske, *Chem. Eur. J.* **1996**, *2*, 1292.
[16] G. S. Hanan, J.-M. Lehn, N. Kyritsakas, J. Fischer, *J. Chem. Soc., Chem. Commun.* **1995**, 765.
[17] D. M. Bassani, J.-M. Lehn, G. Baum, D. Fenske, *Angew. Chem.* **1997**, *109*, 1931; *Angew. Chem. Int. Ed. Engl.* **1997**, *36*, 1845; D. M. Bassani, J.-M. Lehn, *Bull. Soc. Chim. Fr.* **1997**, *134*, 897.
[18] J.-P. Kintzinger, P. Maltèse, J. Rojo, F. J. Romero-Salguero, J.-M. Lehn, to be published.
[19] H. Günther, *NMR-Spektroskopie*, Georg Thieme Verlag, Stuttgart, **1973**.
[20] J. Rojo, F. J. Romero-Salguero, J.-L. Lehn, unpublished results.
[21] Related species gave emission quantum yields of $< 1.10^{-3}$ and 0.11 for the ligand and the Zn^{II}_4 grid complex, respectively: I. Manet, V. Balzani, D. Volkmer, J.-M. Lehn, unpublished results.
[22] See for example: N. Armoroli, L. De Cola, V. Balzani, J.-P. Sauvage, C. O. Dietrich-Buchecker, J.-M. Kern, A. Bailal *J. Chem. Soc., Dalton Trans.* **1993**, 3241.
[23] Quantum-dot cells, each with four dots of [2 × 2] grid-type, have been used in the realization of multicellular automata: A. O Orlov, I. Ambani, G. H. Bernstein, C. S. Lent, G. L. Snider, *Science* **1997**, *277*, 928; J. Glanz, *Science* **1997**, *277*, 898.
[24] G.M. Sheldrick, *SHELX-97*, University of Göttingen, Germany, **1997**.
[25] E. Keller, *SCHAKAL97*, University of Freiburg, Germany, **1997**.

Received March 8, 1999
[I99090]